International Journal of Research and Review
[Indexed, Peer-Reviewed Journal]
Volume 13; Issue: 1; January 2026
Website: www.ijrrjournal.com
Research Paper *E-ISSN: 2349-9788; P-ISSN: 2454-2237*

Internal Dosimetry with Monte Carlo Code PHITS: Validation of Specific Absorbed Fraction Values for Voxel and Mesh-based Adult Male Phantoms

Asa Pratiwi[1], Wahyu Setia Budi[2], Pandji Triadyaksa[2]

[1]Master of Physics, Diponegoro University, Indonesia
[2]Department of Physics, Faculty of Sciences and Mathematics, Diponegoro University, Indonesia

Corresponding Author: Asa Pratiwi

DOI: https://doi.org/10.52403/ijrr.20260133

ABSTRACT

In targeted radionuclide therapy (TRT), accurate internal dosimetry is crucial for maximizing therapeutic outcomes while minimizing side effects. The Particle and Ion Transport System (PHITS) is more accessible and user-friendly, although Monte Carlo (MC) simulations have become the gold standard in absorbed dose modeling and radiation transport. The purpose of this study is to evaluate the effectiveness of using PHITS version 3.35 (2025) for calculating internal dosimetry parameters and to quantitatively evaluate the differences in SAF values between the ICRP 110 reference voxel-based adult male phantom model and the ICRP 145 reference mesh-based phantom, validated against reference data. Review dosimetric parameters for at least nine source-target organ pairs, including absorbed fraction (AF) and specific absorbed fraction (SAF). This simulation includes monoenergetic photons and electron particles ranging in energy from low (≤0.1 MeV) to high (1 MeV). For most organs, the statistical uncertainty of the computation is kept below 5%. The results show that using a mesh phantom can make the estimation of internal dosimetric parameters such as SAF more anatomically representative. In general, electron SAFs are more sensitive than photon SAFs to differences in organ mass and geometric realism. This is especially true for large organs like the liver and kidneys, which have thin walls and are closely positioned across different organs. As a result, the internal dosimetry estimates produced by the mesh phantom are more anatomically representative than those produced by the voxel phantom.

Keywords: PHITS; Internal dosimetry; Nuclear medicine; Specific absorbed fraction; MRCP; voxelized phantoms

INTRODUCTION

Nuclear medicine therapy and diagnostics utilize radioisotopes linked to specific ligands to selectively deliver radiation to target tissues, such as receptors or tumor antigens. This approach is known as Targeted Radionuclide Therapy (TRT) and has rapidly developed as a precise molecular imaging and therapeutic strategy[1]. After being introduced into the body thru the venous, digestive, or respiratory systems, radiopharmaceuticals will be distributed and accumulate in specific organs or tissues according to the patient's biological characteristics[2]. During its physical and biological half-lives, the radioisotope continuously emits radiation, contributing to the patient's internal radiation exposure.

Internal radiation exposure over time might provide considerable radiobiological hazards

to both target and non-target organs, requiring precise and dependable dose evaluation[3]. The precision of internal dosimetry is essential for assessing clinical risks, enhancing therapeutic efficacy, and safeguarding patient safety, particularly in procedures that involve multiple doses, such as myocardial perfusion imaging or radionuclide therapy[4–6]. Achieving high accuracy in internal dosimetry is contingent upon comprehending and identifying certain dosimetric characteristics that accurately reflect radiation interactions within the human body.

In clinical practice, the average absorbed dose in the target organ (k) is typically computed using a convolution method, which entails multiplying the time-integrated activity in the source organ (h) by the S-value, denoted as $S(k \leftarrow h)$.The S-value denotes the proportion of radiation energy released from the source organ and absorbed by the target organ, contingent upon the radiation type and energy, as well as the anatomical connection between the two organs. The calculation of the S-value is significantly reliant on the Absorbed Fraction (AF) and the Specific Absorbed Fraction (SAF), which are essential factors in internal dosimetry[7]. These parameters can be accurately derived solely by Monte Carlo simulations with computational phantoms that depict human anatomy. Numerous Monte Carlo codes, including MCNP, Geant4, and GATE, have been extensively employed and validated for this objective[7–10].

In addition to the Monte Carlo physics techniques and libraries, the precision of SAF calculations is significantly affected by the type of computational phantom employed. Early-generation phantoms derived from mathematical models (stylized phantoms) exhibit constraints in anatomical fidelity, prompting the creation of voxel-based phantoms as advocated in ICRP Report 110[11]. Despite providing enhanced anatomical realism, voxel phantoms remain constrained in their ability to consistently depict thin-walled tissues. In response, the ICRP presented the Mesh Reference Computational Phantom (MRCP) in ICRP Report 145, facilitating enhanced anatomical modeling with tetrahedral mesh geometry[12,13]. The Monte Carlo code PHITS is increasingly utilized in medical physics and internal dosimetry, featuring a more user-friendly interface and facilitating the use of various phantoms, including personalized ones, which has resulted in the creation of personalized dosimetry systems such as RT-PHITS[7,14,15]. Nonetheless, the systematic validation of the most recent iteration of PHITS (3.35) concerning internal dosimetry, utilizing the ICRP 110 voxel reference phantom, alongside its comparison with the ICRP 145 mesh phantom, remains considerably restricted and has not been thoroughly contrasted with established organ-level reference databases.

This study seeks to assess the feasibility of employing PHITS version 3.35 (2025) for calculating internal dosimetry parameters and to quantitatively analyze the discrepancies in SAF values between the ICRP 110 reference voxel-based adult male phantom and the ICRP 145 reference mesh-based phantom, both validated against sources such as the OpenDose database[16] and the research conducted by M.-G. Lee and C. Park (2026)[14]. The investigation examined self-irradiation and cross-irradiation scenarios at different monoenergetic electron and photon energy levels to assess the impact of variations in anatomical representation and organ mass on the precision of internal dosimetry parameters.

MATERIALS & METHODS

Voxel and mesh computational phantoms of an adult male

CT-based phantoms, particularly voxels, were initially presented in ICRP Report 103 and are deemed more representative for adults compared to the stylized reference models in ICRP Report 89, as they are tailored to the attributes of individual adult males and females[17,18]. Both were represented as voxel phantoms in the later

ICRP Report 110[11]. Additionally, in ICRP Report 133, the phantom shape remained unchanged, but the organ masses were amended to reflect the blood content within each organ[19]. Both models, regardless of mass alterations, equally capture the kinetics and distribution of radiopharmaceuticals at the voxel level, facilitating a more precise evaluation of absorbed dose gradients. The bulk organ regeneration is illustrated in Table 1.

The ICRP 110 article delineates 141 tissues and organs characterized by 53 distinct densities and particular atomic compositions, which were computed and categorized into 25 sub-planes. In contrast to the male phantom, which consists of around 7 million voxels, the female phantom contains about 14 million voxels. The increased voxel count facilitates superior spatial sampling in comparison to the male phantom. The attributes of the adult male reference phantom are based on a CT scan of a 38-year-old individual. The adult male is characterized by dimensions of 254 x 127 x 222 voxels, each measuring 2.137 x 2.137 x 8.0 mm, resulting in a height of 1.76 m and a weight of 73 kg. The phantom matrix data files were obtained from the additional material included in the ICRP 110 report[11,16].

Table 1. Phantom voxel organ mass and mesh of adult male

ID Organ ICRP 145	Organs/tissue	Mass (kg)		R. diff in organ mass
		ICRP 110	ICRP 145	
7000	*Gall bladder wall*	0.014	0.010	-29%
7100	*Gall bladder contents*	0.054	0.058	7%
8700	*Heart wall*	0.330	0,386	17%
8800	*Blood in heart chamber*	0.500	0.510	2%
8900~9400	*Kidney left cortex, Kidney left medulla, Kidney left pelvic, Kidney right cortex, Kidney right medulla, Kidney right pelvic*	0.310	0.422	36%
9500	*Liver*	1.800	2.360	31%
11300	*Pancreas*	0.140	0.174	24%
12000~12100	*Salivary glands, left & right*	0.084	0.088	5%
12700	*Spleen*	0.150	0.228	52%
13700	*Urinary Bladder wall*	0.050	0.050	0%
13800	*Urinary Bladder contetnt*	0.200	0.200	0%

The paramount advancement occurred with the release of ICRP Publication 145: Adult Mesh-Type Reference Computational Phantoms (MRCP) in 2020. It is designated as a phantom hybrid due to its amalgamation of voxel and parameterized methodologies, employing mesh-based (or boundary) surface representations to accurately illustrate the contours of human organs[13]. MRCP may accurately depict human anatomical contours with exceptional precision, eliminating the staircase effect typically observed in voxel models. From an anthropometric standpoint, the male phantom measures 176 cm in height and weighs 73 kg, and the female phantom stands at 163 cm and weighs 60 kg; both are constructed with millions of triangular and tetrahedral pieces, yielding exceptional detail and geometric precision. Figure 1 illustrates the blood mass content with organ mass updates, based on elevated reference values for male MRCP with a height of 176 cm and weight of 73 kg, and female MRCP with a height of 163 cm and weight of 60 kg. The male phantom comprises 2.5 million triangles in PM format and 8.2 million tetrahedra in TM format, whereas the female phantom contains 2.6 million triangles in PM format and 8.6 million tetrahedra in TM format[12].

The primary benefit of MRCP is its geometric adaptability. The mesh structure enables the modification, deformation, or

personalization of organs while preserving the integrity of their anatomical shapes, rendering it exceptionally appropriate for the rigorous demands of contemporary Monte Carlo dosimetry, which requires intricate and high-resolution modeling[13]. This model can accurately depict the spatial interactions of organs, including inter-organ spacing and irregular organ forms, hence enhancing the precision of radiation transport and absorbed dose calculations. Some microscopic structures, including minuscule tissue formations (e.g., the ocular lens) and exceedingly thin tissue layers (e.g., the stem cell layer in gastric wall mucosa and intestinal epithelium), remain constrained in their modeling capabilities[14]. Nonetheless, the MRCP is the most accurate and thorough phantom in comparison to earlier ICRP models.

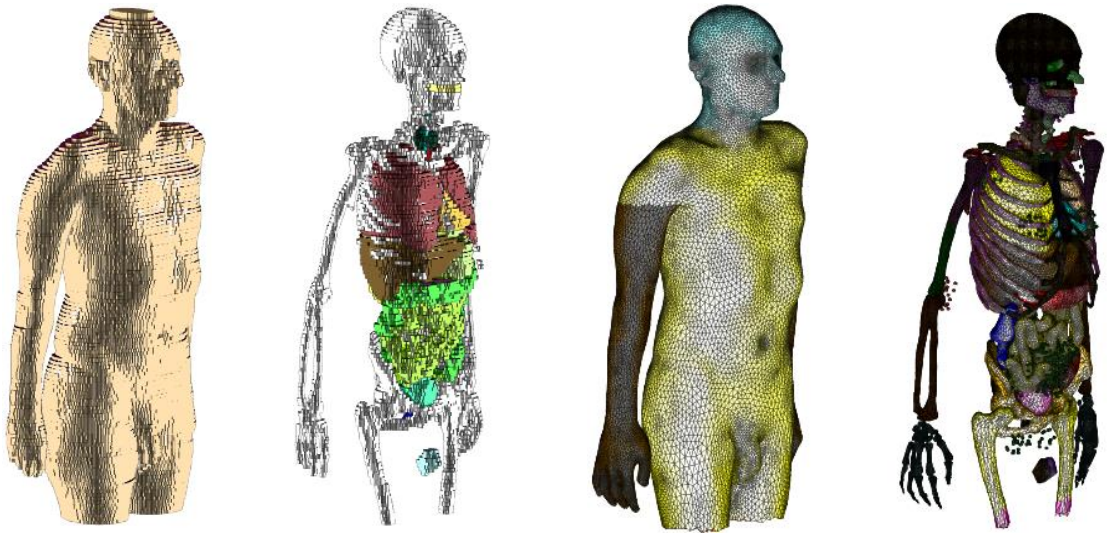

(a) (b) (c) (d)

Figure 1. (a) The ICRP 110 and (b) the ICRP 145 adult male reference phantom of the extremity were generated in this study using PHITS 3.35, showing the skin (right) and visible vital organs and bones (left).

This study focuses on the use of the adult male reference phantom models from ICRP reports 110 and 145, standardized by Tatsuhiko Sato (format 15/04/2025) and implemented in PHITS, with the upper extremities truncated as shown in Figure 1. This approach aims to optimize computational time without affecting the results.

Radiation Transport Simulation Code and Simulation Parameters

PHITS. The simulation was conducted utilizing PHITS version 3.35, which was updated in April 2025. PHITS, equipped with a superior random number generator and accurate dose estimate features, is ideally suited for internal dosimetry applications[20]. Enhanced functionalities, including adjustable energy cutoff and parallelization support (≥3.17 version), optimize AF calculations for small organs and augment computational efficiency on multicore platforms[21]. The transport of electrons and photons is simulated using the integrated EGS5 algorithm, which utilizes a track structure method for low-energy electrons (≤0.1 MeV) to consider secondary ionization, Bremsstrahlung, and elastic scattering, thus enhancing accuracy in low-energy interactions. The most recent manual for version 3.35 by Ogawa et al. (2024) describes PHITS as a multifaceted radiation transport algorithm that emphasizes the path structure model. The trajectory structure calculation is a technique employed to simulate the motion of charged particles, explicitly accounting for each of their atomic

interactions. This calculation effectively assesses the damage inflicted by radiation on small-scale nanostructures, including DNA and chromosomes[22].

Over the course of three months (September–November 2025), this study was carried out at the Al-Barkah computing unit of the Faculty of Science and Mathematics, Diponegoro University, Indonesia. A single window operating in OpenMP Application Programming Interface (API) parallel computing mode [$OMP=0] was used for the PHITS simulation (1 PC: CPU Ryzen 5900XT, 16 GB RAM). 64 cores were used to execute the PHITS simulation, allowing for an effective simulation runtime without compromising simulation outcomes. In accordance with ICRU guidelines, the source was first modeled with a particular energy on an organ/tissue model using two different adult male phantom models: one based on the ICRP report 110 reference voxel model and the other on the ICRP report 145 reference mesh-based adult male phantom model. In a certain area or organ, known as the source organ (h) in relation to the target region or organ (k), monoenergetic electron and photon particles from the source are uniformly dispersed. Reviewing electron and photon particles at monoenergetic changes of 0.05, 0.1, and 1 MeV allowed for the execution of simulations. Then, in order to determine the associated uncertainty, computational recording was carried out utilizing [T-Deposit] computations to output AF and SAF values along with statistical fluctuations in the particle history.

Parameter dosimetry

The absorbed fraction (AF) $\phi\ (k \leftarrow h)$ denotes the ratio of the energy E_0 radiated from the source region h to the energy absorbed E in the target region k:

$$\phi(k \leftarrow h) = \frac{E}{E_0} \quad (1)$$

The specific absorbed fraction (SAF) $\Phi\ (k \leftarrow h)$ is defined as the ratio of the absorbed fraction to the mass of the target organ m_k:

$$\Phi(k \leftarrow h) = \frac{\phi(k \leftarrow h)}{m_k} \quad (2)$$

Database as a reference

Validation was done to make sure the simulation parameters were appropriate for use before comparing the two adult male phantom models, ICRP 110 and ICRP 145, namely voxel and mesh, using separate versions of PHITS 3.35.

Open Dose. An open-access nuclear medicine dosimetry database is provided by the international collaborative database, which consists of 18 teams from 30 institutions. This project calculates average SAFs from different MC using six well-known Monte Carlo codes (EGSnrc, FLUKA, GATE, Geant4, MCNP/MCNPX, and PENELOPE) based on the reference phantom model with adult female and male genders from ICRP Report 110. S-values can also be obtained using decay data from ICRP 107, which contains 1,252 radioisotopes, based on the average values from the SAF database. Under a Creative Commons license, all data is publicly available via the www.opendose.org website[16].

M.-G. Lee and C. Park (2026). Using PHITS 3.34 on male and female adult MRCP phantoms based on ICRP report 145 and the Korean mesh-type reference phantom (MRKP). Determining SAF as an internal dosimetry parameter. Assuming a homogenous photon distribution within each source organ, the simulation results for the SAF of different photon energies (0.1, 1, and 10 MeV) were obtained for a number of source organs, including the thyroid, liver, gallbladder, and heart wall. This work uses the MRCP phantom to show how PHITS can be used for contemporary dosimetry calculations[14].

STATISTICAL ANALYSIS

Carmer (1946) employed the propagation method to calculate the relative differences and their associated uncertainties[23,24]. The SAF values derived from PHITS 3.35 simulations using mesh-based phantom model variations (x) and voxel-based

phantom models as a reference (y) are compared using the following formula:

$$R\% = \left(\frac{y-x}{y}\right) \times 100\% \quad (3)$$

In contrast, the propagation approach was used for the SAF value in the uncertainty value of the relative difference R, specifically σ_R. The partial derivative of the absolute uncertainty of the SAF value derived mesh-based phantom model (σ_x) and the absolute uncertainty of the SAF values derived voxel-based phantom models as reference (σ_y) were used as examples:

$$\frac{\partial R}{\partial x} = \frac{1}{y}, \frac{\partial R}{\partial y} = -\frac{x}{y^2} \quad (4)$$

Therefore, the uncertainty of σ_R was defined as follows:

$$\sigma_R = \sqrt{\left(\frac{1}{y} \cdot \sigma_x\right)^2 + \left(\frac{x}{y^2} \cdot \sigma_y\right)^2} \quad (5)$$

RESULT

Over source/target organ configurations were calculated concurrently utilizing PHITS version 3.35. Utilized 100 million to 1 billion particle histories and achieved an optimal relative uncertainty of less than 5% for both self-irradiation and cross-irradiation scenarios. This simulation necessitates an average of 6 hours per CPU for monoenergetic electrons (0.05, 0.1, and 1.0 MeV) and 2.5 hours per CPU for monoenergetic photons (0.05, 0.1, and 1.0 MeV) utilizing the ICRP 110 reference voxel phantom. The ICRP 145 reference mesh phantom simulation necessitates approximately 120 hours per CPU for monoenergetic electrons (0.05, 0.1, and 1.0 MeV) and 48 hours per CPU for monoenergetic photons (0.05, 0.1, and 1.0 MeV).

Validation of the SAF phantom voxel against reference

The Open Dose database provides results for the ICRP 110 adult male and female models, multiple source/target pairs, and monoenergetic electron-photon particles. Their findings can be juxtaposed with those of this experiment, which involved a reduced sample size; however, it is noteworthy that both investigations utilized the mean values of the SAF derived from multiple simulations, including MC Geant 10.5, Gate 8.1, and PMM. Three monoenergetic levels (0.05, 0.1, and 1.0 MeV) for electrons and photons can be compared.

The average relative difference of SAF (R_{SAF}) and its relative uncertainty (σ_R) were computed to validate PHITS 3.35 in comparison to the OpenDose database utilizing the ICRP 110 adult male phantom model. In the self-absorption scenario, the measurements for the two configurations are as follows: (-0.21 ± 0.02) % for 0.05 MeV electrons; (-0.03 ± 0.03) % for 0.1 MeV electrons; and (-0.31 ± 0.03) % for 1 MeV electrons. Additionally, the values for photons are (0.18 ± 0.33) % for 0.05 MeV; (-0.63 ± 0.21) % for 0.1 MeV; and (-2.41 ± 0.47) % for 1 MeV. The cross-absorption case for monoenergetic electrons across nine configurations is (-2.69 ± 7.00) % at 0.05 MeV; (-3.17 ± 2.48) % at 0.1 MeV; and (1.34 ± 0.91) % at 1 MeV. The cross-absorption case for monoenergetic photons across 13 configurations is (1.17 ± 1.91) % at 0.05 MeV; (0.38 ± 0.84) % at 0.1 MeV; and (0.23 ± 0.66) % at 1 MeV. The outcomes for a reduced number of cases are displayed in Table 2 and Table 3.

Table 2. Validation of our work with data published in OpenDose database[16] *Electron*

E_{el} (MeV)	Open Dose		This Work	
	SAF (/kg)	σ SAF	SAF (/kg)	σ SAF
Liver ← Liver				
0.05	5.55×10^{-1}	0.001%	5.56×10^{-1}	0.000%
0.1	5.55×10^{-1}	0.001%	5.55×10^{-1}	0.000%
1.0	5.35×10^{-1}	0.015%	5.36×10^{-1}	0.000%
Liver ← Kidney				
0.05	2.34×10^{-5}	1.18%	2.30×10^{-5}	0.58%

0.1	7.43×10^{-5}	4.20%	7.50×10^{-5}	0.45%
1.0	1.85×10^{-3}	0.39%	1.81×10^{-3}	0.14%
Liver ←Gall Bladder content				
0.05	1.67×10^{-4}	0.59%	1.68×10^{-4}	0.28%
0.1	5.30×10^{-4}	0.15%	5.40×10^{-4}	0.38%
1.0	1.68×10^{-2}	0.54%	1.75×10^{-2}	0.05%

Table 3. Validation of our work with data published in OpenDose platform[16] Photon

E_{ph} (MeV)	Open Dose		This Work	
	SAF (/kg)	σ_{SAF}	SAF (/kg)	σ_{SAF}
Liver ← Liver				
0.05	1.74×10^{-1}	0.23%	1.74×10^{-1}	0.01%
0.1	1.00×10^{-1}	0.20%	1.01×10^{-1}	0.01%
1.0	8.39×10^{-2}	0.36%	8.52×10^{-2}	0.01%
Liver ← Kidney				
0.05	3.64×10^{-2}	0.41%	3.63×10^{-2}	0.03%
0.1	2.58×10^{-2}	0.47%	2.58×10^{-2}	0.02%
1.0	1.90×10^{-2}	0.30%	1.90×10^{-2}	0.02%
Liver ←Gall Bladder content				
0.05	1.47×10^{-1}	0.06%	1.47×10^{-1}	0.01%
0.1	8.70×10^{-2}	0.17%	8.67×10^{-2}	0.01%
1.0	6.60×10^{-2}	0.35%	6.62×10^{-2}	0.01%

Verification of the SAF phantom mesh against reference

The research conducted by M.-G. Lee and C. Park (2026) served as a benchmark for corroborating the simulation with the ICRP 145 reference adult male MRCP phantom model. Validation is conducted on a limited number of instances, specifically involving photon particles with two monoenergetic energy levels. Owing to the restricted availability of source-target organ configurations in the reference. The findings are displayed in Table 4.

Table 4. Validation of our work with data published in M.-G. Lee and C. Park (2026)[14] *Photon*

E (MeV)	M.-G. Lee and C. Park		This Work	
	SAF	σ_{SAF}	SAF	σ_{SAF}
Liver ← Liver				
0.1	8.53×10^{-2}	0.01%	8.54×10^{-2}	0.01%
1.0	7.07×10^{-2}	0.02%	7.15×10^{-2}	0.01%
Salivary Gland ← Liver				
0.1	4.24×10^{-4}	1.40%	4.24×10^{-04}	0.43%
1.0	8.43×10^{-4}	1.10%	8.21×10^{-04}	0.68%
Liver ← Gall Bladder content				
0.1	7.78×10^{-2}	0.01%	7.58×10^{-2}	0.03%
1.0	5.99×10^{-2}	0.02%	5.69×10^{-2}	0.02%

Comparison of phantom voxel and mesh by PHITS 3.35

Upon validation, the SAF for the mesh and phantom voxels was utilized as a reference for comparison. This study analyzes self and cross irradiation instances for both electron and photon particles to ascertain the distinctions in contour and organ mass factors between the two phantom models. Figure 2 illustrates self-irradiation, whereas Figure 3 and Figure 4 depict cross-irradiation in general and in detail, respectively.

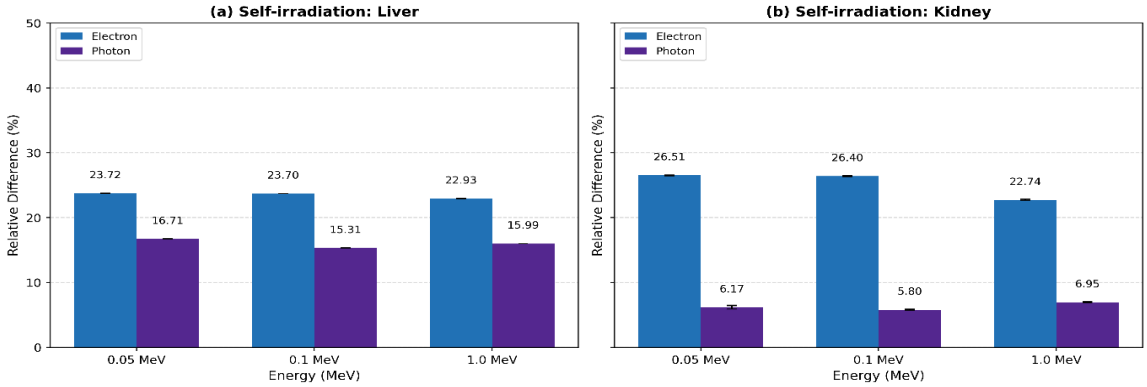

Figure 2. Relative differences SAFs of the ICRP 145 mesh phantom model against the ICRP 110 voxel (taken as reference) calculated with PHITS 3.35 for monoenergetic electron and photon emissions of 0.05, 0.1, and 1.0 MeV, for (a) Liver and (b) Kidney as source organs in the case of self-irradiation

The average value of R ± σ_R SAFs was calculated as a validation of the ICRP 145 reference adult male phantom against the ICRP 110 reference using PHITS 3.35. For the self-absorption case, the values for the two configurations are (25.12 ± 0.02) % for 0.05 MeV electrons; (25.05 ± 0.03) % for 0.1 MeV electrons; and (22.84 ± 0.04) % for 1 MeV electrons, as well as (11.44 ± 0.06) % for 0.05 MeV photons; (10.55 ± 0.05) % for 0.1 MeV photons; and (11.47 ± 0.05) % for 1 MeV photons. The cross-absorption case for monoenergetic electrons from 10 configurations is (31.13 ± 3.64) % for 0.05 MeV; (33.24 ± 2.02) % for 0.1 MeV; and (-9.99 ± 1.91) % for 1 MeV. The cross-absorption case for monoenergetic photons from 13 configurations is (6.14 ± 0.86) % for 0.05 MeV; (3.92 ± 0.36) % for 0.1 MeV; and (3.03 ± 0.29) % for 1 MeV.

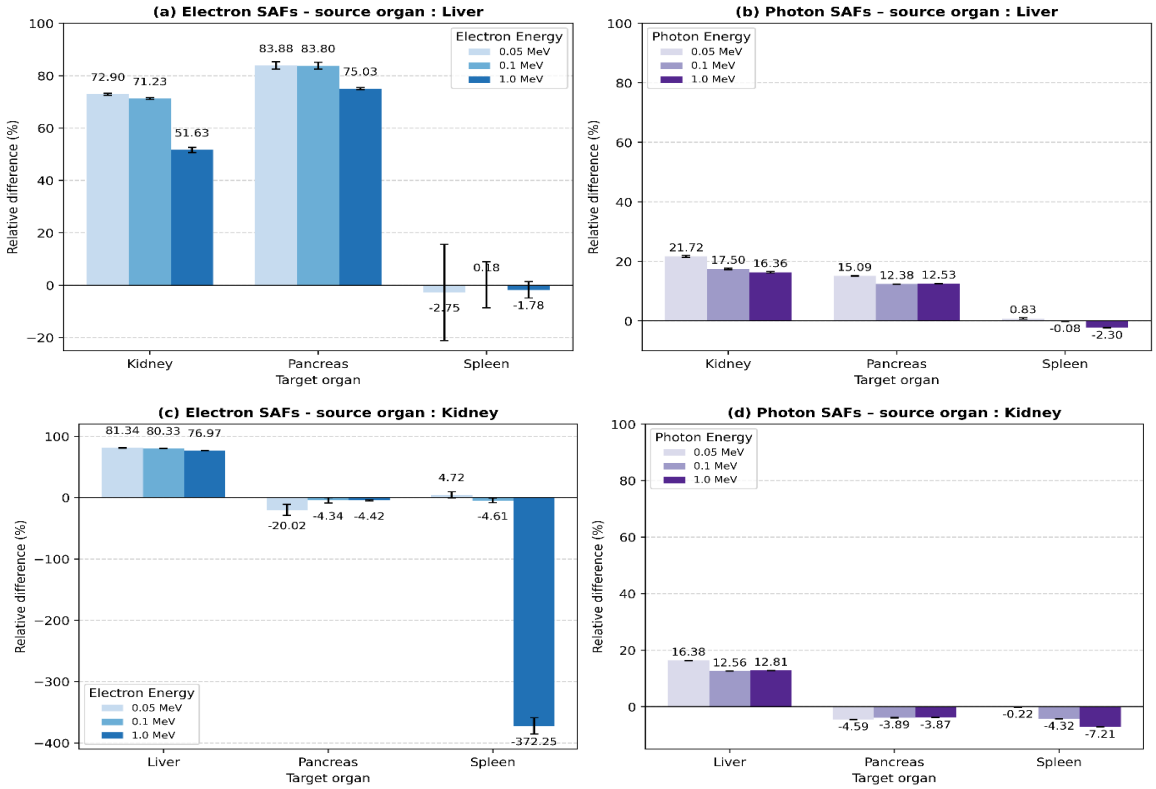

Figure 3. Relative differences between SAFs of the ICRP 145 mesh phantom model against the ICRP 110 voxel (taken as reference) calculated with PHITS 3.35 for monoenergetic electron and photon emissions of 0.05, 0.1, and 1.0 MeV in the case of cross-irradiation. (a) SAFs electron and (b) SAFs photon with Liver as source organs, (c) SAFs electron and (d) SAFs photon with Kidney as source organ

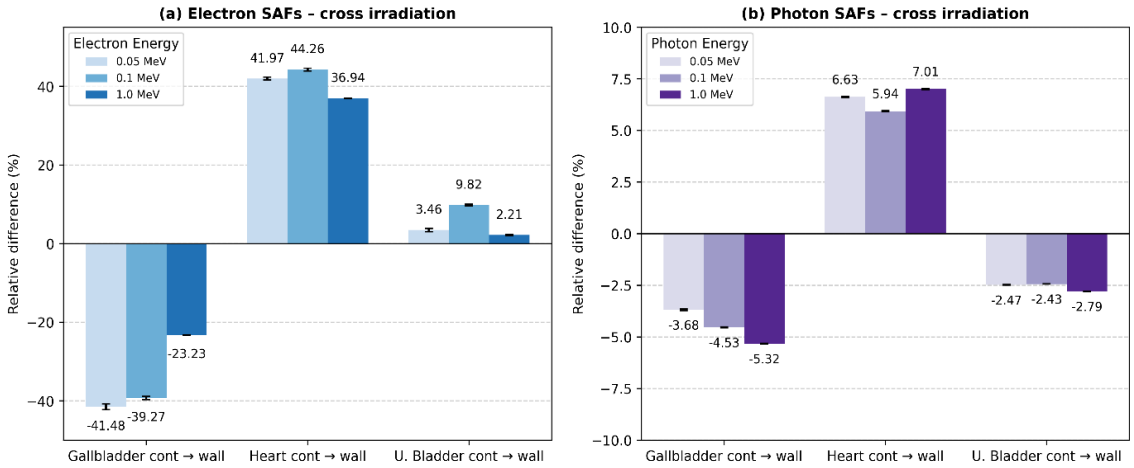

Figure 4. Relative differences between specific absorption fractions (SAFs) of the ICRP 145 mesh phantom model against the ICRP 110 voxel (taken as reference) calculated with PHITS 3.35 for monoenergetic (a) electron and (b) photon emissions of 0.05, 0.1, and 1.0 MeV, for special case of hollow organs case of cross-irradiation

DISCUSSION

This study evaluates the viability of PHITS v3.35 for internal dosimetry and quantitatively contrasts SAFs between ICRP 110 voxel and ICRP 145 mesh phantoms for self- and cross-irradiation scenarios involving monoenergetic electrons and photons. PHITS 3.35 demonstrates strong concordance with the reference database (OpenDose) and prior research M.-G. Lee and C. Park (2026), making it suitable for advanced internal dosimetry parameter calculations (S-value). Nonetheless, notable systematic discrepancies exist in certain instances, highlighting the constraints of the phantom model's sensitivity to anatomical accuracy.

Validation against OpenDose and comparison with M.-G. Lee and C. Park are displayed in Table 2, Table 3, and Table 4, showed excellent agreement for photons (relative differences generally <1%) and good agreement for many cases of electron self-irradiation (e.g., Liver←Liver). Nevertheless, some electron cross-irradiation configurations showed larger deviations (>2–3%), while statistical uncertainties remained low (<1%), indicating that the differences were systematic and related to geometric assumptions and the physical settings of the simulation [16].

Fundamental physical factors include the impact of organ mass and thickness on SAF and the distinction in energy transfer and deposition between electrons and photons. The increase in electron SAF differences (~22–24% and ~22–26.5%, respectively) in the mesh phantom can be explained by the increase in liver mass (~31%) and kidney mass (~36%), as the SAF is inversely proportional to the target mass under self-irradiation conditions (Figure 2). Changes in relative position, wall layer thickness, and surface shape have a significant impact on electrons with very short ranges for cross-irradiation (Figure 3 and Figure 4); this causes significant deviations (e.g., differences of ~70–85% for some source–target pairs at an energy of 0.05–0.1 MeV, and a change in sign in the case of the spleen with an increase in mass of ~52%), especially at high energies (1 MeV). Even though there are simply variations in the organ's geometric shape, the relative differences in mass are rather significant (2–10%) even if the target organs are thin and do not experience mass changes like the bladder wall[7]. On the other hand, because of their penetration and Compton scattering, which disperses energy more broadly, photons show significantly lower sensitivity[11,12,25].

From a methodological standpoint, these results imply two useful implications: (1)

mesh representations that maintain continuous thickness significantly reduce SAF bias compared to voxels for thin-walled organs and near-field cross-irradiation scenarios (e.g., kidney walls, renal walls, and heart walls); (2) SAF results are sensitive to the choice of simulation parameters (e.g., energy cut-off, cross-sections, and secondary particle tracking), so dosimetric studies should go beyond the generally regarded as reliable PHITs 3.35. However, the local accuracy of electrons is highly dependent on geometric realism and the physical settings required to control the trade-off between accuracy and computational time.

The use of a monoenergetic spectrum rather than a complete radionuclide spectrum, the selection of an energy cut-off range for computational efficiency, and the concentration on a reference phantom without taking patient or population-specific phantom variances into account are the limitations of this study. In order to reduce systematic bias in internal dosimetry, it is advised to: (i) investigate the sensitivity of transport parameters and energy cut-offs; (ii) run simulations using clinical radionuclide spectra, such as emitters; (iii) examine the effects of therapeutic choices and clinical S-values; and (iv) employ mesh phantoms or hybrids for thin-walled hollow cases.

CONCLUSION

This study aims to investigate the influence of anatomical discrepancies and mass variations between the ICRP 110 voxel phantom and the ICRP 145 mesh phantom, utilizing an adult male model, on the specific absorbed fraction (SAF) values for monoenergetic photons and electron particles in both self-irradiation and cross-irradiation scenarios. The results demonstrate that the MC PHITS simulation method employed in this study is scientifically valid, as it aligns with established references and the laws of particle transport physics. The comparison of mesh and voxel models as references demonstrates the reliance of SAF on particle mass, distance, and range. Consequently, electron SAFs exhibit significantly more sensitivity to the geometric realism of organ structures and variations in mass compared to photon SAFs. Consequently, employing a phantom mesh yields a more anatomically accurate assessment of internal dosimetry. This work illustrates that the establishment and utilization of patient-specific internal dosimetry parameters are essential and can facilitate further research into more clinically pertinent and individualized dosimetry modeling.

Declaration by Authors

Acknowledgement: The Japan Atomic Energy Agency (JAEA) granted access and permission to use the PHITS code for this study (ID 2025-0194).

Source of Funding: This project was supported by the Indonesian Education Scholarship (BPI). BPI is jointly funded by Center for Higher Education Funding and Assessment, Ministry of Higher Education, Science, and Technology of Republic Indonesia and Endowment Fund for Education Agency, Ministry of Finance of Republic Indonesia

Conflict of Interest: No conflicts of interest declared.

REFERENCES

1. Dash A, Sudipta C, Ambikalmajan PMR, et al. Peptide receptor radionuclide therapy: an overview. Cancer Biother Radiopharm 2015;30(2).
2. ICRP. ICRP Publication 141: Occupational Intakes of Radionuclides: Part 4. Ann ICRP 2019;48(2–3):9–501.
3. Eberlein U, Cremonesi M, Lassmann M. Individualized Dosimetry for Theranostics: Necessary, Nice to Have, or Counterproductive? Journal of Nuclear Medicine 2017;58(Supplement 2):97S-103S.
4. Henzlova MJ, Duvall WL, Einstein AJ, et al. ASNC imaging guidelines for SPECT nuclear cardiology procedures: Stress, protocols, and tracers. Journal of Nuclear Cardiology 2016;23(3):606–39.
5. Ramonaheng K, Staden JA van, Raan H du. Accuracy of two dosimetry software programs for 177Lu radiopharmaceutical

therapy using voxel-based patient-specific phantoms. Heliyon 2022;8(7).
6. Tiantian L, Edwin A, Bieke L, et al. Quantitative Imaging for Targeted Radionuclide Therapy Dosimetry - Technical Review. Theranostics 2017;7(18).
7. Villoing D, Marcatili S, Garcia MP, et al. Internal dosimetry with the Monte Carlo code GATE: validation using the ICRP/ICRU female reference computational model. Phys Med Biol 2017;62(5):1885.
8. Bhar M, Kadri O, Manai K. Assessment of self- and cross-absorbed SAF values for HDRK-man using Geant4 code: internal photon and electron emitters. Nucl Sci Tech 2019;30(10).
9. Hadid L, Desbrée A, Schlattl H, et al. Application of the ICRP/ICRU reference computational phantoms to internal dosimetry: calculation of specific absorbed fractions of energy for photons and electrons. Phys Med Biol 2010;55(13):3631.
10. Lamart S, Simon SL, Bouville A, et al. S values for 131I based on the ICRP adult voxel phantoms. Radiat Prot Dosimetry 2016;168(1):92–110.
11. ICRP. ICRP Publication 110: Adult Reference Computational Phantoms. Ann ICRP 2009;39(2):1–164.
12. ICRP. ICRP Publication 145: Adult Mesh-Type Reference Computational Phantoms. Ann ICRP 2020;49(3):13–201.
13. Oliver S, Cases J, Juste B, et al. Determination of organ doses in thyroid treatments with radioactive iodine by Monte Carlo simulation. Radiation Physics and Chemistry 2024; 221:111737.
14. Lee MG, Park C. Feasibility of the PHITS code for calculating specific absorbed fraction values in internal dosimetry. Radiation Physics and Chemistry 2026; 238:113168.
15. Sato T, Furuta T, Sasaki H, et al. Establishment of a practical methodology for evaluating equieffective dose of individual patients based on RT-PHITS. EJNMMI Physics 2025;12(1):28.
16. Chauvin M, Borys D, Botta F, et al. OpenDose: open access resources for nuclear medicine dosimetry. J Nucl Med 2020;61(10):1514–9.
17. ICRP. Basic anatomical and physiological data for use in radiological protection: reference values: ICRP Publication 89. Annals of the ICRP 2002;32(3):1–277.
18. ICRP. The 2007 Recommendations of the International Commission on Radiological Protection. J Radiol Prot 2007;11(3):199–203.
19. ICRP. The ICRP computational framework for internal dose assessment for reference adults: specific absorbed fractions. ICRP Publication 133. Ann ICRP 2016;45(2):5–73.
20. Sato T, Iwamoto Y, Hashimoto S, et al. Features of Particle and Heavy Ion Transport Code System (PHITS) version 3.02. J Nucl Sci Technol 2018;55(6):684–90.
21. Shiiba T, Kuga N, Kuroiwa Y, et al. Evaluation of the accuracy of mono-energetic electron and beta-emitting isotope dose-point kernels using particle and heavy ion transport code system: PHITS. Appl Radiat Isot 2017; 128:199–203.
22. Ogawa T, Yuho Hirata, Yusuke Matsuya, et al. Overview of PHITS Ver.3.34 with particular focus on track-structure calculation. EPJ - Nuclear Sciences & Technologies 2024;10.
23. Theodorsson E. Understanding and expressing variation in measurement results. J Lab Precis Med 2025;10(1).
24. Cramer H. Mathematical Methods Of Statistics. Princeton, NJ: Princeton University Press.; 1946.
25. Bolch WE, Eckerman KF, Sgouros G, et al. MIRD Pamphlet No. 21: A Generalized Schema for Radiopharmaceutical Dosimetry—Standardization of Nomenclature. J Nucl Med 2009;50(3):477–84.

How to cite this article: Asa Pratiwi, Wahyu Setia Budi, Pandji Triadyaksa. Internal dosimetry with Monte Carlo code PHITS: validation of specific absorbed fraction values for voxel and mesh-based adult male phantoms. *International Journal of Research and Review*. 2026; 13(1): 351-361. DOI: *10.52403/ijrr.20260133*

******